Arno H. A. Stienen
Research Assistant of Department of
Biomechanical Engineering,
University of Twente,
Enschede, The Netherlands;
Research Associate of Department of Physical
Therapy and Human Movement Sciences,
Northwestern University,
Chicago, IL 60611
e-mail: arnostienen@gmail.com

Edsko E. G. Hekman
Research Associate
Department of Biomechanical Engineering,
University of Twente,
Enschede, The Netherlands 7500 AE

Gerdienke B. Prange
Research Assistant
Roessingh Research and Development,
Enschede, The Netherlands 7522 AH

Michiel J. A. Jannink
Cluster Manager of Roessingh Research and
Development,
Enschede, The Netherlands 7522 AH;
Assistant Professor of Department of
Biomechanical Engineering,
University of Twente,
Enschede, The Netherlands 7500 AE

Arthur M. M. Aalsma
Director
BAAT Medical,
Hengelo, The Netherlands 7553 LZ

Frans C. T. van der Helm
Full Professor of Department of Biomechanical
Engineering,
University of Twente,
Enschede, The Netherlands 7500 AE;
Full Professor of Department of Biomechanical
Engineering,
Delft University of Technology,
Delft, The Netherlands 2600 AA

Herman van der Kooij
Associate Professor of Department of
Biomechanical Engineering,
University of Twente,
Enschede, The Netherlands;
Associate Professor of Department of
Biomechanical Engineering,
Delft University of Technology,
Delft, The Netherlands 7500 AE

Dampace: Design of an Exoskeleton for Force-Coordination Training in Upper-Extremity Rehabilitation

The Dampace exoskeleton combines functional exercises resembling activities of daily living with impairment-targeted force-coordination training. The goal of this paper is to evaluate the performance of the Dampace. In the design, the joint rotations are decoupled from the joint translations; the robot axes align themselves to the anatomical axes, overcoming some of the traditional difficulties of exoskeletons. Setup times are reduced to mere minutes and static reaction forces are kept to a minimum. The Dampace uses hydraulic disk brakes, which can resist rotations with up to 50 N m and have a torque bandwidth of 10 Hz for multisine torques of 20 N m. The brakes provide passive control over the movement; the patients' movements can be selectively resisted, but active movement assistance is impossible and virtual environments are restricted. However, passive actuators are inherently safe and force active patient participation. In conclusion, the Dampace is well suited to offer force-coordination training with functional exercises. [DOI: 10.1115/1.3191727]

1 Introduction

Patient-friendly robots for upper-extremities rehabilitation are used as diagnostic and therapeutic aids for a wide range of disabilities. After a stroke, improving limited arm function is needed to regain functional abilities. Current rehabilitation robots try to accomplish this using a number of different rehabilitation strategies. For example, the MIT-Manus [1,2] assists arm movements during task execution when deemed necessary, the MIME [3] mirrors the movement of the unaffected to the affected arm, the ACT-3D [4] tackles undesired abnormal muscle couplings, and the ARMin [5] motivates patients by interacting with virtual environments. Overall, these robots make rehabilitation therapy more challenging for the patients and less labor intensive for the therapists, and supply the physicians, therapists, and the scientific community with more objectively gathered data.

According to systematic reviews, the new robot assisted therapies are at least as good as regular therapy for stroke rehabilita-

tion. van der Lee et al. [6] tentatively concluded that the type of therapy matters less than the exercise intensity. Several approaches with and without robots resulted in roughly the same effect when the level of intensity was matched. They indicated that using robots may be a useful way for increasing the intensity. Platz [7] found evidence for superior treatment efficacy of task oriented, motor-relearning programs and giving different patient subgroups specific training strategies. Also, a higher intensity of motor rehabilitation resulted in an accelerated, although not necessarily better, motor recovery. Finally, two recent reviews [8,9], concluded that robot assisted therapy of the shoulder and elbow improves motor control of these joints, and probably more than conventional therapy. But consistent influence on the functional abilities of the patients was not found. These four systematic reviews agree with the main principle of motor learning; the improvement in motor-control performance is directly linked with the amount of practice done [10]. However, improved motor control is not necessarily the same as an increased functional ability.

The results with rehabilitation robots are in line with reviews on conventional upper-extremity therapy. The latter indicate that intensive and task-specific exercises, consisting of active, repetitive movements, give the best results [11–13]. Actively generating movements requires more brain activity and results in better motor learning than externally-powered arm movements [14]. For severely affected stroke patients, active participation can be facilitated by reducing the gravitational pull on the arm, as found in previous studies [15–17].

As an alternative to the strict functional and task-specific approach, Dewald and co-workers [4,18–23] used impairment-targeted movements to achieve improved motor control in stroke rehabilitation. Their multidegree-of-freedom force-coordination training tackles a commonly identified cause of stroke patients' movement disorders: the abnormal coupling between the elbow and shoulder joint torques [24,17].

Other groups of intervention with support in literature, with less focus on activities of daily living, are the targeted movement-coordination training [25], progressive resistance strength training, and force-coordination training [26–34]. Yet, on the latter two approaches, the evidence is not conclusive [35]. The combination of functional exercises with dynamic, high-intensity resistance training looks promising [36]. Additionally, training by actively resisting the patients' movements may also stimulate them to generate more appropriate movement patterns when emphasizing the movement error [37,38]. General motor learning theories, on which these theories are partly based, are thought to be useful for motor recovery after stroke [39–41].

Combining these approaches, a training device was needed, which could help identify causes behind the movement disorders of stroke patients, tackle these causes with isolated force-coordination training over multiple joints, and integrate the isolated training into a functional, task-specific training protocol. In the training stages active patient participation is essential, and by offering interesting training environments and varying the levels of difficulty, patients should stay motivated and challenged. Therefore, we created our dynamic force-coordination trainer for the upper-extremities: the Dampace.

The goal of this paper is to evaluate the performance of the Dampace. The device should increase exercise intensity, stimulate active patient participation, allow most functional movements of daily living, offer selective control over joint rotations, and be practical for rehabilitation therapy. This study expands on an earlier conference publication [42].

2 Requirements and Implications

Robot interaction with the upper-extremities is possible with endpoint manipulators, exoskeletons, and cable suspensions. Endpoint manipulators have a single connection to the hand, wrist, or forearm [3,4,43–45], thereby indirectly controlling joint rotations. Exoskeletons are external skeletons placed over the arm and pow-

ered by actuators on the joints [5,46–50], offering direct control possibilities on these joints at the cost of more complex mechanics. Cable suspensions [51–53] link one or more cables to the arm, increasing both control options and complexity with every additional cable linkage. Due to the limited interaction possibilities, the cable suspensions are ignored in the remainder of this section.

Control over the limb movements with the above devices can be achieved via active actuators or passive brakes. If active assistance of movement is not necessary, then controlled passive brakes offer the advantage of a greater torque-to-weight ratio and inherent safety.

The choices between these devices and actuators are discussed in this section in relation to the device requirements. These requirements were refined with the help of several physicians, therapists, and researchers in The Netherlands.

2.1 Need for Active Assistance of Movement. Most of the current rehabilitation robots are actively powered and designed to assist arm movements when needed [2,54–56]. However, when comparing the training of unassisted reaching to reaching assisted by a rehabilitation robot, equal gains in the range of motion were found [57]. Second, providing too much assistance may negatively influence the motor relearning as patients become less actively involved [58]. Third, increasing the therapy intensity can be achieved without active assistance. And finally, even the evidence of beneficial effects of passive stretching on spasticity in stroke is inconclusive [59]. All of this indicates that for motor relearning in stroke rehabilitation, active actuators may not always be necessary. For instance, force-coordination and error-enhanced training do not depend on active actuation. They can also be realized by brakes applying resistance torques on the joints. With such passive actuators, limb movements may still be facilitated by adding scalable weight support to the device [4,15,16,19,2,1,60]. Weight support only facilitates movements, but does not complete them, keeping the patients actively involved [58,61].

Using controlled resistance has the advantages of inherent safety and a lightweight implementation. Disadvantages are the inability to actively complete movements and create virtual environments, which need external energy. A resistive device requires a separate weight-support mechanism for itself and the human limb. But as the weight-supporting torques at the shoulder can easily exceed 10 N m, even many actively powered devices use separate weight-support mechanisms (see, for example, the Gentle/s [45], the Pneu-WREX [47], and the ARMin [5]). Therefore, if active assistance is not necessary, passive brakes are preferred over active actuators. Both endpoint mechanisms and exoskeletons can be fitted with brakes or actuators.

2.2 Control and Range of Limb Movements. To exercise most functional activities of daily living, the required ranges of motion for the shoulder and elbow joints are defined according to Table 1. In these activities, both the 3D position of the hand and the exact orientation of the limbs are important. For instance, for object grasping movements, the shoulder and elbow angles depend on the position and the type of object. The arm approaches a cup of water differently than a small object like a coin. Thus for impairment assessments and targeted interventions, control over all degrees of freedom is preferred. Second, the shoulder joint does not only have the three rotational degrees of freedom, it also has two translational degrees. These five degrees of freedom form the shoulder girdle [62]. Humans have voluntary control over the shoulder position, but shoulder elevation rotation is also coupled with vertical shoulder translation [65,66]. A rehabilitation device should, at a minimum, not restrict the coupled translations.

By definition, a three-dimensional endpoint device is not able to independently control all four axes of shoulder and elbow simultaneously. To do so, additional fixed (ACT-3D) or controlled rotational degrees of freedom (MIME) are needed. Exoskeletons can give full independent control of all four axes of the joints, but their axes need to be aligned closely to the anatomical axes. They

Table 1 Desired range of motion and maximum resistance torques for shoulder and elbow axes. Defined according to ISB recommendations [62] for respective thoracohumeral and humeroulnar joints. These values are the results of structured interviews with physicians, therapists, and human movement scientists in The Netherlands. The values for the range of motion are compatible with three of the four main categories of movements for activities in daily living [63,64]: touching the contralateral shoulder, touching the mouth (drinking), and touching the head (combing hair); however, the fourth category—moving the hand to the back pocket—is just out of reach.

Joint axis	Range of motion (deg)	Resistance torques (N m)
Shoulder plane of elevation	0–135	25
Shoulder negative elevation	0–120	25
Shoulder axial rotation	−90–0	25
Elbow flexion/extension	0–135	50

do control joint axes directly. And as they closely follow the arm, their dimensions are less dependent on the desired workspace. Endpoint manipulators, by having no axis to align with the human, are less sensitive to (in)voluntary translation of the shoulder than exoskeletons. However, they apply all interaction forces via the hand, potentially creating high reaction forces in the joints. Finally, to match most of the range of motion of the human shoulder and elbow, endpoint manipulators need to cover a large workspace, resulting in a larger device. Overall, exoskeletons offer better control over the measurements of joint movements, have a greater range of motion, and have less joint reaction forces. But care must be taken to align their axes correctly to prevent painful human-robot interaction.

2.3 Usability in Rehabilitation Therapy. For the device to be useful in therapy, some usability issues need to be addressed. The device has to be safe, comfortable, and easy to use and set up. An appealing design will help with patient acceptability. Patient motivation is enhanced by providing stimulating training environments.

Inherent safety is achieved by having controlled resistance instead of active assistance. Endpoint manipulators are comfortable when they do not move the endpoint out of the human range of motion. For exoskeletons, correct joint alignment and translations in the shoulder joint are important. For most of the current devices, the endpoint manipulators are easier in use compared with the exoskeletons due to the longer setup times of the latter. Exoskeletons exist, which do not require their axes to be aligned to the human axes [67]. This minimizes the difference in setup times and reduces some unwanted reaction forces in human joints. Stimulating gaming environments can be created with endpoint manipulators and exoskeletons. Overall, the usability of endpoint manipulators is slightly better.

2.4 Overall Implications. Taken together, combining a self-aligning exoskeleton with controlled brakes at the joint axis results in an inherently safe force-coordination trainer. The combination can make therapeutic movements selectively more intensive and has good control over limb orientations with a large range of motion. To facilitate arm movements, a separate weight-support system is needed. This should, at a minimum, support the weight of the device, but preferably also a scalable amount of arm weight. Joint torques and rotations should be precisely measured for impairment assessments and use in active feedback control.

3 Design and Validation

After evaluating several concepts, the Dampace was created (see Figs. 1–3). The rotations of the three joint axes of the shoulder and the one of the elbow can be actively resisted with the
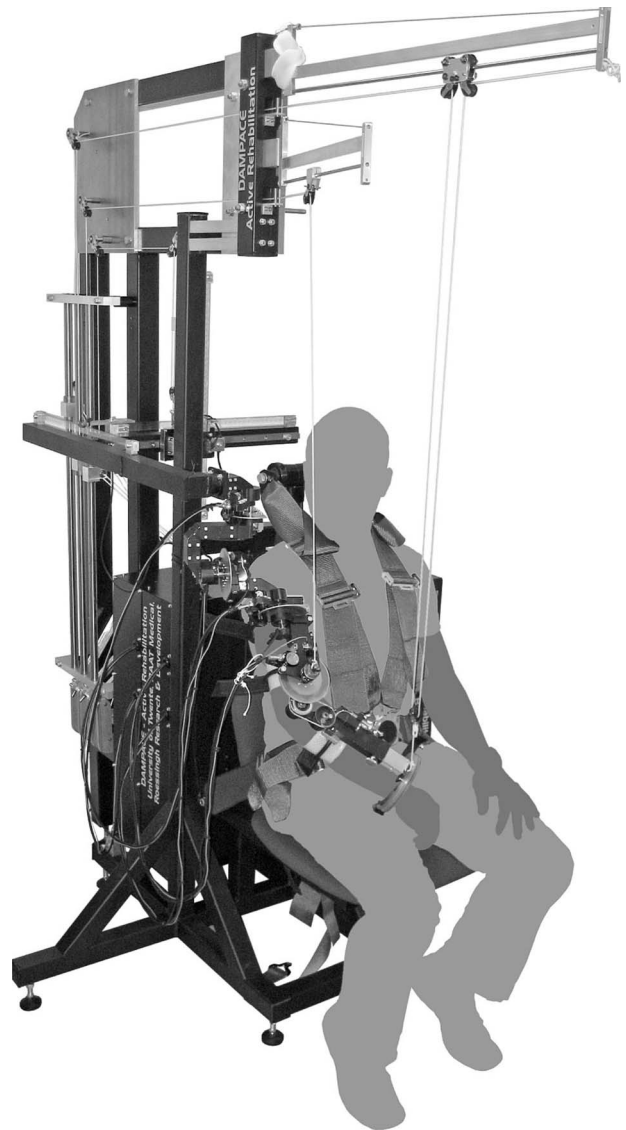
Fig. 1 Dampace: dynamic force-coordination trainer. Powered hydraulic disk brakes on the rotational axes of the shoulder and elbow can apply controlled resistance torques. Additional translating degrees of freedom at the shoulder and elbow self-align the exoskeleton axes to the anatomical axes, and allow full freedom of translation of the shoulder.

hydraulic disk brakes. Additional mechanisms in the exoskeleton auto-align the exoskeleton joints to the human joints. This also gives the shoulder full freedom of translation in any direction. The resistances are applied as pure torques, reducing reaction forces in the shoulder and elbow joints. The weight of the exoskeleton is compensated by an overhanging cabling system connected to a balanced spring mechanism. Finally, feedback control is based on the state of the arm, which is determined via measurements of joint rotations and torques.

3.1 Joint Alignment. In most other exoskeletons, close alignment of exoskeleton and arm axes is a necessity and can be time-consuming to achieve. Rotation of misaligned axes is only possible by internal movements in the musculoskeletal system, full body and trunk movements, or by deforming the soft human tissue. The misalignments also create potential painful reaction forces [68], especially for those with sensitive tissue or sensory problems.

The Dampace overcomes these problems by having the exosk-
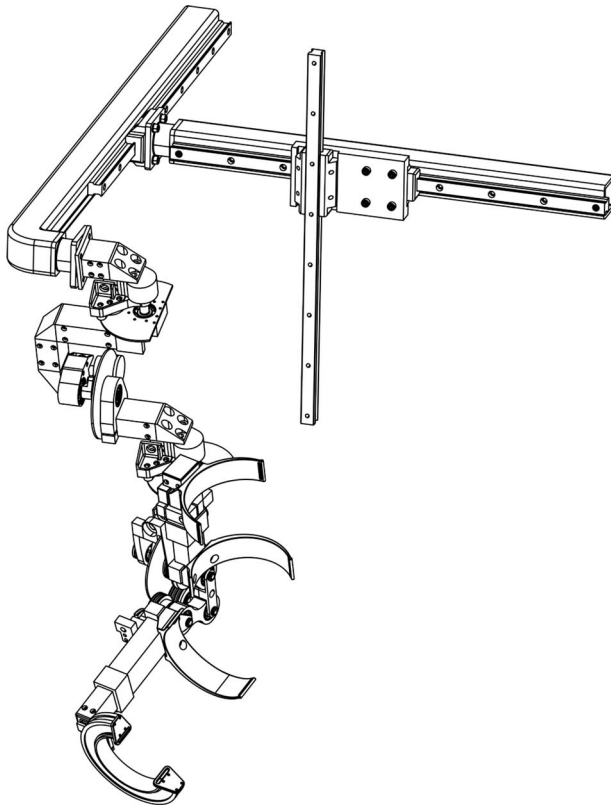
Fig. 2 Sketch of the Dampace exoskeleton and linear guidance mechanism

eleton axes align themselves to the human shoulder and elbow axes (see Figs. 4 and 5 and Ref. [69]). The translations and rotations of the joints are now decoupled. The exoskeleton is connected to the global reference frame via linear guidance system consisting of three perpendicular sliders, each of which can move
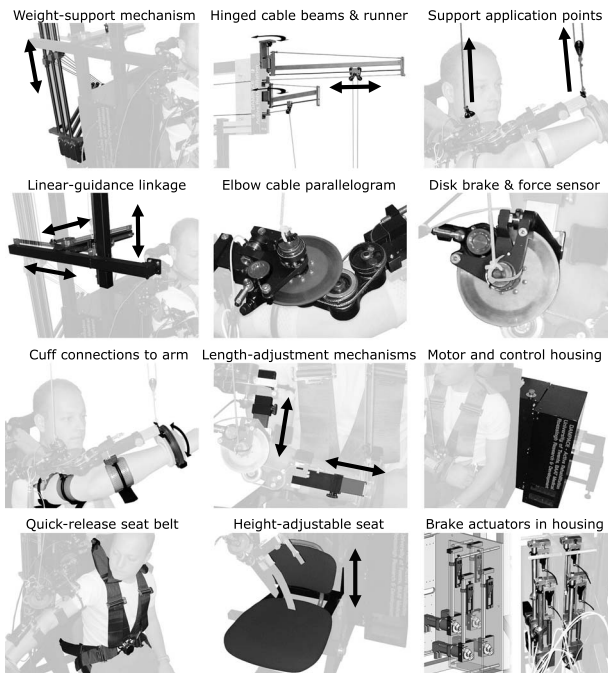
Fig. 3 Collage of Dampace components
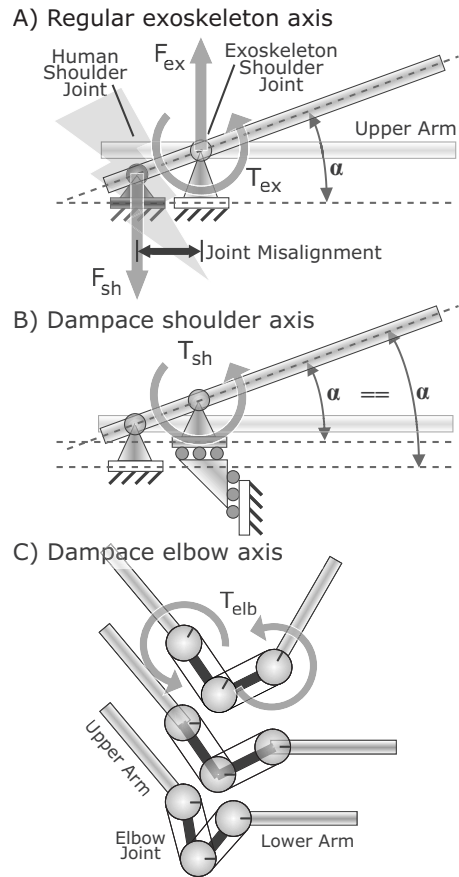
Fig. 4 Axes alignment in exoskeletons: (*a*) **the effects of a single misaligned axis at the shoulder. Due to exoskeleton torque T_{ex}, the arm and exoskeleton axes rotate an angle α. If these axes are misaligned, the human joint has to translate relative to the exoskeleton axis. If the axes are fixed, this movement creates a residual shoulder force F_{sh}, depending on the stiffness of the skin and bone, and an equal exoskeleton reaction force F_{ex};** (*b*) **translating exoskeleton axes prevent these misalignment forces. If a misalignment causes a force F_{ex}, the exoskeleton translates until this force is gone. Torques can be applied to the limb from the rotational-stiff linkage mechanism. In 3D, the effects are the same, with adding the two other rotational axes requiring only one additional linear axis;** (*c*) **the Dampace elbow joint has two extra links, on top of which a parallelogram of cables transfer the forearm orientation to the upper arm. Translation of the joint is now independent of the rotation and vice versa, removing the requirement for the elbow alignment. At the upper arm, the rotation can be controlled and measured; a torque applied here runs through the cables and drum mechanism and is applied to the forearm without causing reaction forces.**

freely over a range of 400 mm. As this linkage is rotational stiff, shoulder joint torques can be still be applied onto the human limb. These torques do not generate the misalignment forces as seen in other exoskeletons. If these forces occur, the passive linkage would translate until they are reduced to zero. However, impedance forces due to inertia of the exoskeleton and friction of the linkage will still cause reaction forces. The inertia of the linkage and exoskeleton was measured to be 8 kg for vertical translations, 7 kg for sideways translations, and 5 kg for forward/backward translations. Each of the three linear-motion rail and sliders (SKF, 15 mm profile rail) adds 4–20 N of static friction to the impedance, depending on the torsional load on the slider. These values will be reduced in future versions by a redesign of the linkage, for instance, with a linkage similar to the Delta robot [70].

The Dampace elbow joint consists of a short two-beam linkage.
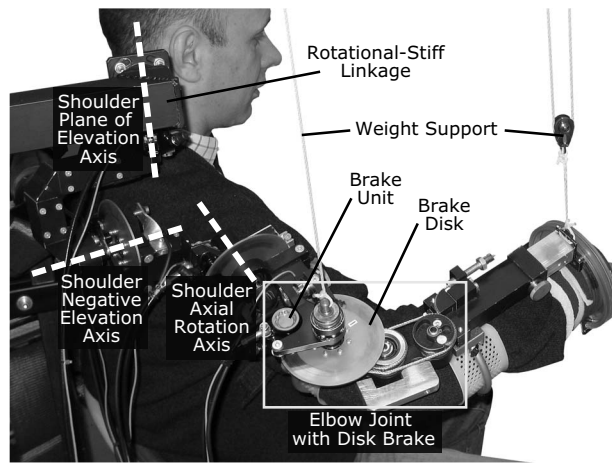
Fig. 5 Shoulder and elbow axes of the Dampace. The three shoulder axes run parallel to the plane of elevation, negative elevation, and axial axis in Table 1. The Dampace negative elevation is positioned at a 90 deg offset on the plane of elevation axes compared with the ISB axes. These axes do not necessarily run through the glenohumeral rotation center, but the movable, rotational-stiff linkage prevents the occurrence of shoulder reaction forces (see Fig. 4).

On top of this, a parallelogram of cables and drums transfer the forearm orientation to the upper arm (see Fig. 4(c)). Translation of the joint is now independent of rotation and vice versa, removing the requirement for close alignment. At the drum on the upper arm, the rotation can be measured and controlled.

The decoupling of the translations and rotations also influences the force interactions between the exoskeleton and human limb. Applying single forces to the limb is now impossible, as the accompanying reaction force would translate the linkage. Instead, the forces must be applied pairwise as torques, requiring two connections to the exoskeleton per limb segment. These additional cuffs are a disadvantage, as it is mounted on the soft outer tissue of the limb and thus reduces the interaction stiffness.

3.2 Hydraulic Disk Brakes. Energy-dissipating resistance torques can be applied via pneumatic, hydraulic, (electro)magnetic, and mechanically passive actuators. Of these, commercially available hydraulic disk brakes have the highest braking torque to weight and size ratio and were thus used in this study. By controlling the internal brake pressure with electromotors in a series elastic configuration [71–75], the amount of resistance can be regulated (see Figs. 6–8). The series elastic configuration makes it possible to use the motor angle in an inner control loop, after which the spring converts the motor angle to a force applied to the brake piston in the handle [76].

The electromotors and drivers used, the LSH050-4-60-320 (nominal torque: 0.7 N m; maximum speed: 6000 rpm) and the CDD32.004C (operating voltage: 230 V; maximum current: 7.2 A), are from LTI Drives. Each motor is combined with a PLE60 gearbox (ratio of 1:20) from Neugart. On the exoskeleton, each axis has a hydraulic mono mini disk brake from Hope Technology, combined with a L1657 load sensor (capacity: 2224 N) from FU-TEK Advanced Sensor Technology. The load sensors signals are conditioned by a SG-3016 isolated strain gauge input module from ICP DAS. The rotation of the three shoulder axes are measured by three off-the-shelf potentiometers, while the elbow axis was measured by the quadrature encoder (resolution: 2500 CPR) from U.S. Digital, consisting of a transmissive rotary code wheel (outer dimension: 2 in.; inner dimension: 1 in.) and a separate encoder module (EM1). The 3D position of the base of the exoskeleton is measured by linear quadrature encoders from U.S. Digital (resolution: 250 CPI), consisting of a transmissive linear strip
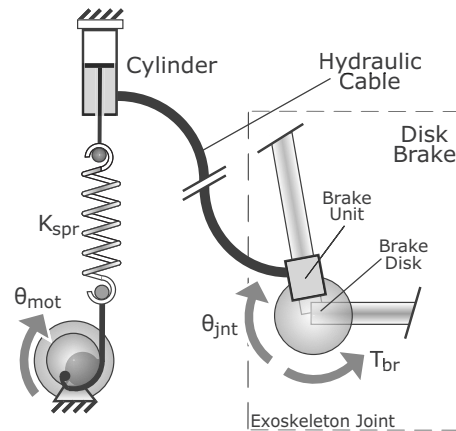
Fig. 6 Disk brake as used on the exoskeleton joints, powered by a series elastic actuator (SEA) mounted on the base frame. The rotation of the motor θ_{mot} is converted by the spring with stiffness K_{spr} and the cylinder to a pressure in the hydraulic cable. This pressure is used to control the braking torque T_{br} on the exoskeleton joint. Note that the braking torque is always in the opposite direction of the joint velocity θ_{jnt}.

and a separate encoder module (EM1) over the full length of the three beams of the linkage. All analog and digital signals run through three shielded printer cables from the Dampace robot to a separate controller station with the computers.

Note that due to the passive brake mechanism, the measured brake torque T_{br} is a complex function of the internal brake pressure and the torque exerted by the human arm T_{arm}. When the arm is inactive, no torques are present in the system and thus none can be measured. With the arm active, the measure brake torque T_{br} is the minimum of the arm torque T_{arm} and the set brake torque. These nonlinearities of the measured brake torque T_{br} make the closing of the middle torque control loop unstably variable.

In experiments with a constant brake pressure in a disk brake, varying the joint velocity from almost zero to the maximum arm velocity caused, at most, 10% variation on the braking torque.
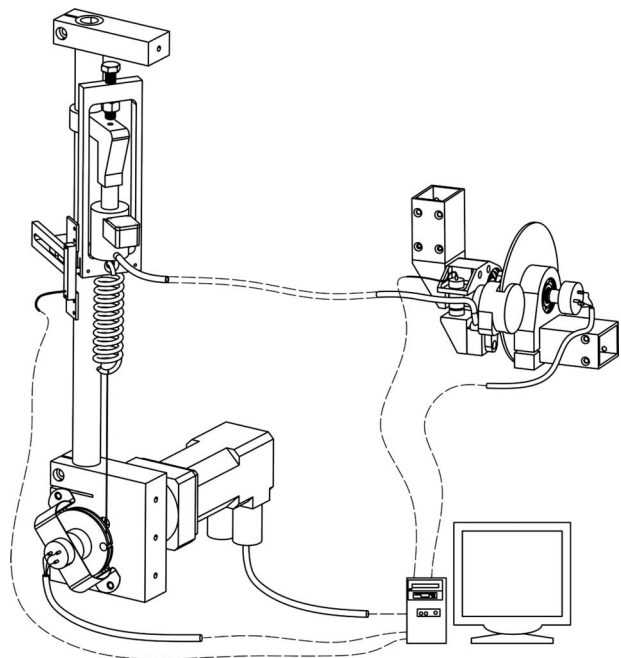
Fig. 7 Sketch of the disk brake as implemented on the negative elevation axis of the shoulder
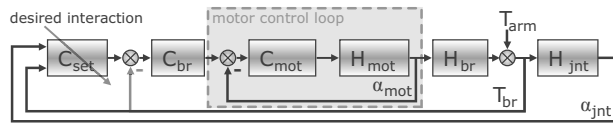
Fig. 8 Control loop for a single disk brake (see Fig. 6), with controllers C, physical systems H, torques T, and angles α. Subscripts denote the electromotor mot, disk brake br, and exoskeleton joint jnt. C_{set} are the desired interaction settings, based on the measurements of the brake torque and joint angle of all the joints. The measured brake torque T_{br} is a complex function of the set brake torque (by the brake pressure) and the human interaction arm torque T_{arm}, and therefore difficult to use in a control loop.

Because the braking torque is mostly hydraulic-pressure dependent and joint-speed independent, achieving a constant braking torque requires little effort. Based on these results, a feed-forward P-controller was implemented for the brake torque C_{br}, circumventing the inherent difficulties of using the measured brake torques F_{br} as mentioned above.

The torque bandwidth was measured using multisine input signals to estimate the frequency response and squared coherence functions of the system in Fig. 8. The functions were estimated with cross- and autospectral densities $S(s)$ of input (i) and output (o) [77,78]. The input signal consisted of 80 summed sines with an observation time of 256 s, spaced logarithmically from 0.1 Hz to 100 Hz, and having a constant power spectral density and random phase shifts. Measurements were repeated four times with four different multisine signals and the results averaged in the frequency domain over four frequencies and four repetitions. For a black-box system with single input and output, the estimated frequency response function $C(s)$ and squared coherence function Coh(s) are

$$C(s) = \frac{S_{io}(s)}{S_{ii}(s)} \qquad (1)$$

$$\mathrm{Coh}(s)^2 = \frac{|S_{io}(s)|^2}{(S_{ii}(s) * S_{oo}(s))} \qquad (2)$$

The frequency response function $C(s)$ is an estimate for the dynamics of the black-box system. The squared coherence function Coh(s) is a measure for the signal to noise ratio and thus the linearity of the system. The squared coherence ranges from 0 to 1, with 1 meaning no nonlinearities or time-varying behavior are present.

Although the brakes are rated by up to 200 N m, the dynamics of the chosen electromotors limit the actual braking torque to 50 N m with a bandwidth of 10 Hz for multisine torques up to 20 N m (see Fig. 9). These amplitude and bandwidth values allow for good positional and torque control of the exoskeleton axes. Speed-dependent resistance, i.e., needed for isokinetic control, is more difficult to accurately achieve at high levels of torque and speed. Finally, contrary to the presence of residual resistance torques in other actuators like electromotors and magnetorheological dampers [79–81], the achievable minimal impedance with disk brakes is zero. The only impedance torques exerted on the arm come from the inertia of the exoskeleton, not the brakes.

3.3 Weight Support. The weight-support forces come from three independent balanced spring mechanisms at the base of the Dampace (see Fig. 10), similar to our earlier Freebal weight-support system [53]. The three mechanisms deliver constant forces to the base of the exoskeleton, the elbow and the wrist. The cable beam is vertically hinged roughly above the human shoulder, which, together with the small slider underneath the cable beam, positions the weight support exactly over the wrist and elbow. To reduce swinging oscillations, a small damper was added to the hinge of the cable beam.

The worm-wheel slider in the spring beam alters the spring attachment point on the beam (see Fig. 10, length R_1), which linearly changes the compensation force $F_{c,b}$ according to Ref. [53].

$$F_{c,b} = F_{sp,z} \frac{R_1}{R_2} = kA \frac{R_1}{R_2} \qquad (3)$$

where $F_{sp,z}$ is the component of the spring force in the vertical direction, R_1 is distance from the spring beam rotation axis to the spring attachment point on the beam, and R_2 is the length of the projected spring beam. The vertical spring force $F_{sp,z}$ is equal to the spring stiffness k times the distance between the spring beam axis and the spring attachment point on the base. This attachment point must be located directly beneath the beam axis. Furthermore, the spring must behave like a zero-length spring; that is, the
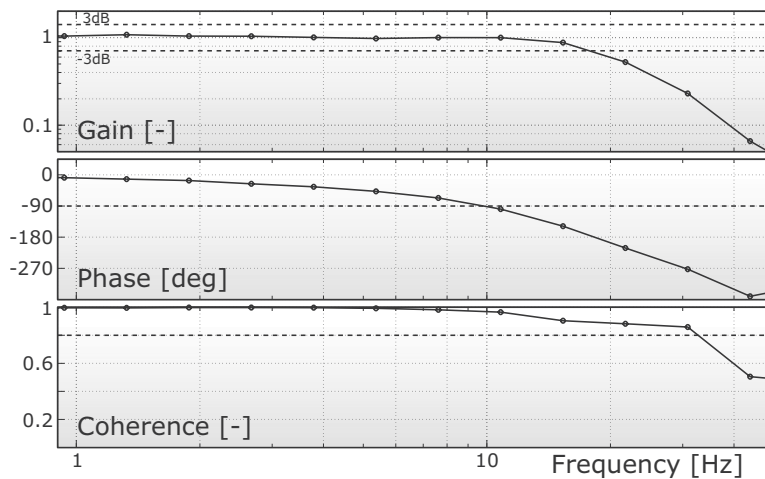
Fig. 9 Torque bandwidth for a 20 N m multisine reference signal, with the frequency response function from the reference torque T_{ref} to the measured torque T_{br}. The −3 dB gain bandwidth is 18 Hz, and the −90 deg phase bandwidth is 10 Hz. The effects of the 2 m long hydraulic cable are seen by the rapidly increasing phase delay. The transport delay in the cable was found to be 5 ms.
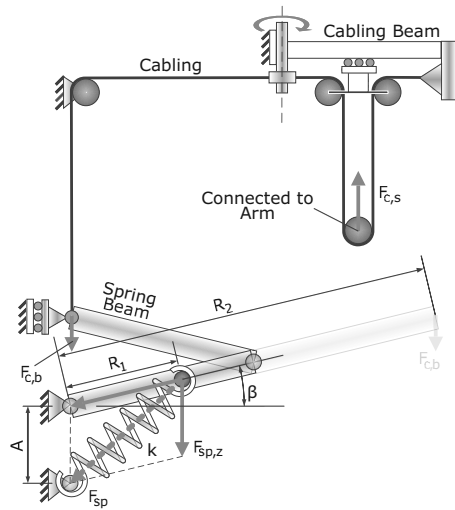
Fig. 10 Weight-support mechanism. The Dampace has three weight-support mechanisms, operating independently of each other and connected to the exoskeleton linkage, the elbow and the wrist. The weight-support force $F_{c,b}$ at the end of the split spring beam is independent of the spring beam angle β for all angles, because the decompositioned spring force F_{sp} in the z-direction ($F_{sp,z}$) is always equal to distance A times the spring stiffness k. As $F_{c,b}=F_{sp,z}R_1/R_2$, the amount of weight support can be altered by changing the spring attachment distance R_1. The weight-support force on the sling $F_{c,s}$ here is equal to $2F_{c,b}$ in a working volume, as defined in Table 1. The cabling beam is vertically hinged roughly above the human shoulder, which, together with the small slider underneath the cabling beam, positions the weight support exactly over the wrist and elbow.

Fig. 11 Measured accuracy of the reconstructed fingertip position. The healthy subject was seated in front of the long side of the $600\times400\times300$ mm³ rectangular frame and asked to trace it with his fingertip. The black stripped lines represent the frame, the dark gray lines the actual trace, and the light gray lines the shadow projections of the trace. The starting position of the fingertip was at the solid black ball, with the upper arm pointing downward and the forearm forward. The lower front and right hand corners were difficult to trace due to the arm and exoskeleton being obstructed by the trunk of the subject and the ribs of the rectangular frame. In general, the fingertip was reconstructed within 20 mm of the actual position.

spring force must change linearly with the spring deflection Δl_{sp} and be zero at zero spring length l_{sp} [82].

$$F_{sp} = k_{sp}\Delta l_{sp}$$

$$F_{sp} = 0 \quad \text{when} \quad l_{sp} = 0 \qquad (4)$$

The needed amount of weight support is dependent on the measured weight of the arm. By locking the shoulder elevation and elbow axis (with a horizontal elbow axis orientation) and weighing the torques around these joints, the weight of the arm can be determined. The amount of support is indicated by the moving slider on the long axis of the spring beam.

3.4 Interaction Control. The controllers are programmed in MATLAB SIMULINK (The MathWorks) and compiled to run in an open-source, real-time Linux environment (RTAI) [83–85], with open-source hardware drivers (COMEDI) [86] for the three National Instruments Corporation DAQ devices (analog input: PCI-6034; encoder input: PCI-6602; analog output: PCI-6703) and have real-time logging and graphical user interface possibilities through PYTHON scripts. The controller runs at a minimum of 1000 Hz on a single core Intel Pentium IV computer.

The feedback controller in the Dampace analyzes the measured rotation angles and joint torques of the four exoskeleton axes and the translation of the linkage. It applies resistance torques to the joints based on these measurements and/or the desired torques. Besides this control in the joint space, the Dampace can also calculate endpoint positions and forces in global coordinates. The accuracy of the calculated endpoint properties suffers slightly due to the large number of mechanical components between the global reference frame and wrist or finger.

To calculate the endpoint position, each component has its position and orientation information calculated relative to the previous component. This creates a cascading set of rotation and transformation matrices. The endpoint forces are calculated by measuring the torque at each axis, then dividing these by the perpendicular length of the axis vector to the endpoint and summing the resulting four forces at the endpoint, and accounting for the movement inertia where needed.

To measure the endpoint positional accuracy, a healthy subject traced a $600\times400\times300$ mm³ rectangular frame (see Fig. 11) with the tip of the index finger. The finger was kept stiff and inline with his forearm without using additional aids. Most of the time, the Dampace software reconstructs the tip of the finger within 20 mm of the actual position. The reconstruction was based on the known dimensions of the Dampace and the measurements of the shoulder to elbow and elbow to fingertip lengths. Most problems, especially those in the lower right hand corner and the lower front bar, were due to the subject not being able to touch the frame due to the exoskeleton colliding with the frame or his own body. For control of rehabilitation exercises, this level of accuracy is more than sufficient. It represents the worst case scenario of a large volume to work in, with the finger as a nonstiff pointer.

Unfortunately, the calculated endpoint forces suffer from variable interjoint interference. The measured elbow torque is affected by simultaneous movements against shoulder torques perpendicular to the elbow axis. The shoulder torque influences the elbow measurements by up to 25%. In the final analysis, and after trying several solutions to no avail, the elevated cabling at the elbow (see Fig. 5) seems to be the culprit. The shoulder torques cause some slight deformation of the elbow bearings, thereby increasing or decreasing the tension in the elevated cabling. To solve this problem, the cabling either has to be brought inline with the elbow joint—thus between the bearings instead of above them—or replaced by push-pull parallelograms. With no perpendicular loading on the elbow joint, the sensor measures the brake torques correctly and the above endpoint force calculation results in the correct endpoint force vector.
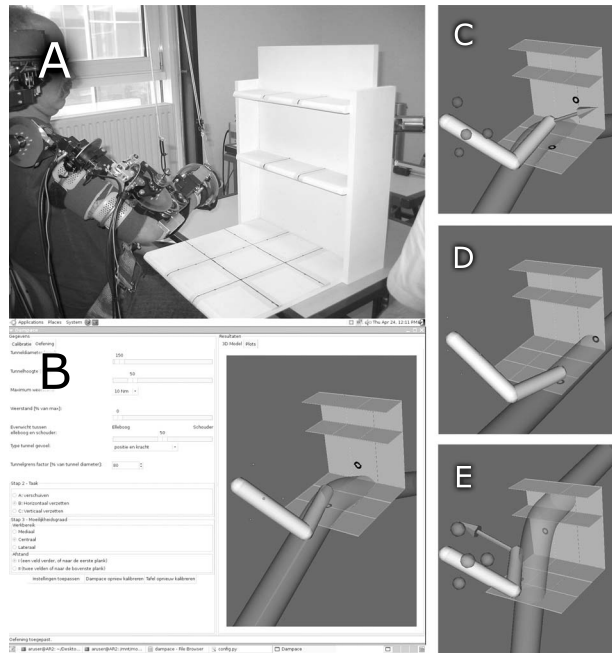
Fig. 12 (*a*) Resistance training setup and (*b*) user interface, where the table of the real-world environment (*a*) is recreated in the computer to allow virtual control (*b*)–(*e*). Patients need to move real objects, sometimes just sliding, or in other times, lifting it to shelves by up to the shoulder level. The movements can be made more difficult by increasing the resistance torque on the shoulder and elbow joints, which the therapist can adjust via the user interface. To guide the patient in making the movement, a virtual tunnel is created (*b*). When the hand moves out of the tunnel (*c*), all the disk brakes lock until the direction of the hand force (shown with an arrow) is again aimed toward the tunnel. The desired trajectory can be altered in direction and movement height (*d*), or desired vertical displacement (*e*). The amount of current brake force is indicated by the color and size of the four visible balls, representing the axes of the shoulder and elbow.

Fig. 13 Integrated gaming environment connected to the Dampace torques and movements. Either isometric thoracohumeral-elevation torques or isotone rotations are mapped to the gas paddle in the racing game, and either humeroulnar isometric torques or isotone rotations to the steering wheel. Good coordination of simultaneous shoulder and elbow torques is thus required for good driving control in the game and should motivate the subjects to keep exercising.

4 Patient Interaction

In the full set of identifying the limitations of a specific stroke patient, isolating the problem and combating these with functional or targeted force-coordination exercises, and integrating the achieved improvement back into activities of daily living, the Dampace can make an important contribution. Identification can be helped by determining the active, unrestricted range of motion, the maximum isometric and resisted forces and speeds, or any other combination of active forces and movements, all measured directly in the joint space. In functional or targeted force-coordination exercises, the controller can apply resistance to specific parts of the movement. This can both restrict or guide the arm to stay inside a desired movement space or make a movement harder to do, thereby increasing the training intensity (see Fig. 12). Finally, at the end of the rehabilitation process, the isolated and targeted training exercises can be gradually integrated into fully functional movements. Thus a force-coordination training to increase the arm strength and control of, for example, an extended arm can be turned into manipulating real objects in a kitchen type of environment. The posture of the forearm also influences the sensory input to the motor cortex [87], increasing the importance of allowing the forearm to orient itself correctly for the functional task at hand. In all stages, the hand can be an integral part of the exercises, as it is always left fully usable.

4.1 Virtual Environments. Although an exoskeleton is probably not the best way to achieve perfect haptic feedback, it is possible to simulate some environments. Virtual movements in water require damping, while static friction is needed for lifting a heavy object or movement over a rough surface. More elaborated environments [74,88] with time-, position-, and direction-dependent resistance and damping have less clear real-world synonyms, but could be interesting in studying specific symptoms. Even so, the environments which can be simulated are limited to those which require no energy input to any part of the system. The resistance trainer can only disperse energy, and the applied torques are always working against the rotational direction. Another restriction is the limited bandwidth of the brakes (10 Hz), which makes it impossible to create hard surfaces at the exact locations. These are not needed for most rehabilitation exercises. With all virtual environments, the haptic feedback is transferred from the exoskeleton to the human arm via cuffs to the upper and forearm, and not via the hand. The decomposition of hand forces to the shoulder and elbow torques might be correct, but the "erroneous" tactile connections of the cuffs do influence the haptic sensation.

4.2 Gaming Interface. In another current example, specific training combats the effects of unwanted multijoint muscle synergies [18,19,22], which is important for patients to regain more functional use in their affected side. To motivate subjects, the human movement and force execution are linked to a gaming console (see Fig. 13). Either isometric thoracohumeral-elevation torques or isotone rotations are mapped to the gas paddle in the racing game, and humeroulnar isometric torques or isotone rotations to the steering wheel. Good coordination of simultaneous shoulder and elbow torques is thus required for good driving control in the game and should motivate the subjects to keep exercising. Although this specific game is too demanding for most stroke patients, it gives an impression of possible alternative training environments with targeted impairment-reduction strategies.

5 Discussion

Not needing to align the Dampace axes to the human shoulder and elbow joints overcomes some of the difficulties traditionally associated with exoskeletons. Although it adds more complexity, the reduction in setup time to a few minutes and the absence of most reaction forces in the human joints are major advantages [67,68]. These have been well received by therapists and physicians. Controlled braking instead of actively assisting actuators

has the advantage of inherent safety and always actively participating patients, at the cost of not being able to assist movements or create some virtual environments. The inherent safety is an important aspect to ensure confidence in the device by patients, therapists, and ethical commissions alike.

Early experiments with healthy subjects and stroke subjects showed that the attention paid to the self-alignment of the axes and reducing the friction in the linkage and weight-support system was well spent. Still, the linkage is about four times heavier as desired, and the linear bearings have too much friction. Having the third shoulder axis of the exoskeleton run parallel but with an offset to the axial rotation axis of the human shoulder generates a lot of linkage movement. As these movements lead to large inertial forces, in future designs the orientation of this third axis needs to be reconsidered. Reducing the weight of and friction in the linkage, and also reducing the amplitude of the necessary linkage translations, should reduce the felt impedance forces fivefold. This should bring them close to 1 kg in any direction. Adding the controlled actuators to the linkage in a zero-impedance mode [89] can further reduce these forces. For better measurements of the joint angles during resisted movements, better arm cuffs are needed. These should potentially use more bony landmarks, as some elderly subjects had very soft arm tissue. The lack of interaction stiffness caused the exoskeleton to have angle offsets with the limb when subjected to torques above 25 N m. Finally, with a static device, it was determined that up to 120 N m of static braking force may be needed for isometric measurements with healthy subjects. This is beyond the maximum strength of the Dampace exoskeleton, although the disk brakes could provide these torques.

Although actively controlled resistance may be enough for motor relearning after a stroke, preliminary results of other active robots seems to indicate that properly supplied assistance can help recovery times [2,54–56]. Determining the proper kind of assistance is thus still a matter of current research in motor skill training and adaptive shared control contexts.

6 Conclusion

In conclusion, the Dampace is well suited to offer force-coordination training with functional exercises. It increase exercise intensity for patients by resisting movement. The passivity of the disk brakes forces active patient participation. The flexibility and range of motion of the exoskeleton allow most functional movements of daily living. Specific impairments can be targeted by the selective control over joint rotations. Finally, the decoupling of the joint rotations and translations reduces the setup time and minimize interaction forces, which improve the usability for rehabilitation therapy.

The Dampace can assist in quantifying movement impairments of stroke patients via unrestricted, isometric or isotonic torque measurements. After quantification, the impairments can be targeted with isolated force-coordination training, potentially over multiple joints. In the last step, the isolated training can be slowly transformed into functional, task-specific training protocols.

Acknowledgment

References

[1] Hogan, N., Krebs, H., Sharon, A., and Charnnarong, J., 1995, "Interactive Robotic Therapist," U.S. Patent No. 5,466,213.
[2] Krebs, H., Palazzolo, J., Dipietro, L., Volpe, B., and Hogan, N., 2003, "Rehabilitation Robotics: Performance-Based Progressive Robot-Assisted Therapy," Auton. Rob., 15(1), pp. 7–20.
[3] Burgar, C., Lum, P., Shor, P., and van der Loos, H., 2000, "Development of Robots for Rehabilitation Therapy: The Palo Alto VA/Stanford Experience," J. Rehabil. Res. Dev., 37(6), pp. 663–673.
[4] Sukal, T., Ellis, M., and Dewald, J., 2007, "Shoulder Abduction-Induced Reductions in Reaching Work Area Following Hemiparetic Stroke: Neuroscientific Implications," Exp. Brain Res., 183(2), pp. 215–223.
[5] Nef, T., Mihelj, M., and Riener, R., 2007, "ARMin: A Robot for Patient-Cooperative Arm Therapy," Med. Biol. Eng. Comput., 45(9), pp. 887–900.
[6] van der Lee, J. H., Snels, I. A., Beckerman, H., Lankhorst, G. J., Wagenaar, R. C., and Bouter, L. M., 2001, "Exercise Therapy for Arm Function in Stroke Patients: A Systematic Review of Randomized Controlled Trials," Clin. Rehabil., 15(1), pp. 20–31.
[7] Platz, T., 2003, "Evidence-Based Arm Rehabilitation—A Systematic Review of the Literature," Nervenarzt, 74(10), pp. 841–849.
[8] Prange, G., Jannink, M., Groothuis-Oudshoorn, C., Hermens, H., and IJzerman, M., 2006, "Systematic Review of the Effect of Robot-Aided Therapy on Recovery of the Hemiparetic Arm After Stroke," J. Rehabil. Res. Dev., 43(2), pp. 171–184.
[9] Kwakkel, G., Kollen, B., and Krebs, H., 2008, "Effects of Robot-Assisted Therapy on Upper Limb Recovery After Stroke: A Systematic Review," Neurorehabil. Neural Repair, 22(2), pp. 111–121.
[10] Schmidt, R., and Lee, T., 1999, Motor Control and Learning, 3rd ed., Human Kinetics, Champaign, IL.
[11] Kwakkel, G., Wagenaar, R., Twisk, J., Lankhorst, G., and Koetsier, J., 1999, "Intensity of Leg and Arm Training After Primary Middle-Cerebral-Artery Stroke: A Randomised Trial," Lancet, 354(9174), pp. 191–196.
[12] Barreca, S., Wolf, S., Fasoli, S., and Bohannon, R., 2003, "Treatment Interventions for the Paretic Upper Limb of Stroke Survivors: A Critical Review," Neurorehabil. Neural Repair, 17(4), pp. 220–226.
[13] Feys, H., de Weerdt, W., Verbeke, G., Steck, G., Capiau, C., Kiekens, C., Dejaeger, E., van Hoydonck, G., Vermeersch, G., and Cras, P., 2004, "Early and Repetitive Stimulation of the Arm Can Substantially Improve the Long-Term Outcome After Stroke: A 5-Year Follow-Up Study of a Randomized Trial," Stroke, 35(4), pp. 924–929.
[14] Liu, J., Cramer, S., and Reinkensmeyer, D., 2006, "Learning to Perform a New Movement With Robotic Assistance: Comparison of Haptic Guidance and Visual Demonstration," J. Neuroengineering Rehabil., 3, Paper No. 20.
[15] Prange, G., Jannink, M., Stienen, A., van der Kooij, H., IJzerman, M., and Hermens, H., 2009, "Influence of Gravity Compensation on Muscle Activation Patterns During Different Temporal Phases of Arm Movements of Stroke Patients," Neurorehabil. Neural Repair, 23(5), pp. 478–485.
[16] Prange, G., Kallenberg, L., Jannink, M., Stienen, A., van der Kooij, H., IJzerman, M., and Hermens, H., 2009, "Influence of Gravity Compensation on Muscle Activity During Reach and Retrieval in Healthy Elderly," J. Electromyogr Kinesiol, 19(2), pp. e40–e49.
[17] Brunnstrom, S., 1970, Movement Therapy in Hemiplegia: A Neurophysiological Approach, Harper and Row, New York.
[18] Beer, R., Dewald, J., Dawson, M., and Rymer, W., 2004, "Target-Dependent Differences Between Free and Constrained Arm Movements in Chronic Hemiparesis," Exp. Brain Res., 156(4), pp. 458–470.
[19] Ellis, M., Holubar, B., Acosta, A., Beer, R., and Dewald, J., 2005, "Modifiability of Abnormal Isometric Elbow and Shoulder Joint Torque Coupling After Stroke," Muscle Nerve, 32(2), pp. 170–178.
[20] Beer, R., Ellis, M., Holubar, B., and Dewald, J., 2007, "Impact of Gravity Loading on Post-Stroke Reaching and Its Relationship to Weakness," Muscle Nerve, 36(2), pp. 242–250.
[21] Ellis, M., Acosta, A., Yao, J., and Dewald, J., 2007, "Position-Dependent Torque Coupling and Associated Muscle Activation in the Hemiparetic Upper Extremity," Exp. Brain Res., 176(4), pp. 594–602.
[22] Ellis, M., Sukal, T., DeMott, T., and Dewald, J., 2007, "ACT-3D Exercise Targets Gravity-Induced Discoordination and Improves Reaching Work Area in Individuals With Stroke," Proceedings of the Tenth ICORR '07.
[23] Ellis, M. D., Sukal, T., DeMott, T., and Dewald, J. P. A., 2008, "Augmenting Clinical Evaluation of Hemiparetic Arm Movement With a Laboratory-Based Quantitative Measurement of Kinematics as a Function of Limb Loading," Neurorehabil. Neural Repair, 22(4), pp. 321–329.
[24] Twitchell, T., 1951, "The Restoration of Motor Function Following Hemiplegia in Man," Brain, 74(4), pp. 443–80.
[25] Krebs, H., Mernoff, S., Fasoli, S., Hughes, R., Stein, J., and Hogan, N., 2008, "A Comparison of Functional and Impairment-Based Robotic Training in Severe to Moderate Chronic Stroke: A Pilot Study," NeuroRehabilitation, 23(1), pp. 81–87.
[26] Rutherford, O., 1988, "Muscular Coordination and Strength Training. Implications for Injury Rehabilitation," Sports Med., 5(3), pp. 196–202.
[27] Weiss, A., Suzuki, T., Bean, J., and Fielding, R., 2000 "High Intensity Strength Training Improves Strength and Functional Performance After Stroke," Am. J. Phys. Med. Rehabil., 79(4), pp. 369–376.
[28] Hortobagyi, T., Tunnel, D., Moody, J., Beam, S., and DeVita, P., 2001, "Low- or High-Intensity Strength Training Partially Restores Impaired Quadriceps Force Accuracy and Steadiness in Aged Adults," J. Gerontol., Ser. A, 56(1), pp. B38–B47.
[29] Fasoli, S., Krebs, H., Stein, J., Frontera, W., and Hogan, N., 2003, "Effects of Robotic Therapy on Motor Impairment and Recovery in Chronic Stroke," Arch. Phys. Med. Rehabil., 84(4), pp. 477–482.
[30] Morris, S., Dodd, K., and Morris, M., 2004, "Outcomes of Progressive Resistance Strength Training Following Stroke: A Systematic Review," Clin. Rehabil., 18(1), pp. 27–39.
[31] Ouellette, M., LeBrasseur, N., Bean, J., Phillips, W., Stein, J., Frontera, W., and Fielding, R., 2004, "High-Intensity Resistance Training Improves Muscle Strength, Self-Reported Function, and Disability in Long-Term Stroke Survi-

vors," Stroke, **35**(6), pp. 1404–1409.

[32] Yang, Y., Wang, R., Lin, K., Chu, M., and Chan, R., 2006, "Task-Oriented Progressive Resistance Strength Training Improves Muscle Strength and Functional Performance in Individuals With Stroke," Clin. Rehabil., **20**(10), pp. 860–870.

[33] Ada, L., Dorsch, S., and Canning, C., 2006, "Strengthening Interventions Increase Strength and Improve Activity After Stroke: A Systematic Review," Aust. J. Phys., **52**(4), pp. 241–248.

[34] Kahn, L., Lum, P., Rymer, W., and Reinkensmeyer, D., 2006, "Robot-Assisted Movement Training for the Stroke-Impaired Arm: Does It Matter What the Robot Does?," J. Rehabil. Res. Dev., **43**(5), pp. 619–630.

[35] Bohannon, R., 2007, "Muscle Strength and Muscle Training After Stroke," J. Rehabil. Med., **39**(1), pp. 14–20.

[36] Patten, C., Dozono, J., Schmidt, S., Jue, M., and Lum, P., 2006, "Combined Functional Task Practice and dynamic High Intensity Resistance Training Promotes Recovery of Upper-Extremity Motor Function in Post-Stroke Hemiparesis: A Case Study," J. Neurol. Phys. Ther., **30**(3), pp. 99–115.

[37] Reinkensmeyer, D., Emken, J., and Cramer, S., 2004, "Robotics, Motor Learning, and Neurologic Recovery," Annu. Rev. Biomed. Eng., **6**, pp. 497–525.

[38] Patton, J., Stoykov, M., Kovic, M., and Mussa-Ivaldi, F., 2006, "Evaluation of Robotic Training Forces That Either Enhance or Reduce Error in Chronic Hemiparetic Stroke Survivors," Exp. Brain Res., **168**(3), pp. 368–383.

[39] Poole, J., 1991, "Application of Motor Learning Principles in Occupational Therapy," Am. J. Occup. Ther., **45**(6), pp. 531–537.

[40] Dobkin, B., 2004, "Strategies for Stroke Rehabilitation," Lancet Neurol., **3**(9), pp. 528–36.

[41] Hogan, N., Krebs, H., Rohrer, B., Palazzolo, J., Dipietro, L., Fasoli, S., Stein, J., Hughes, R., Frontera, W., Lynch, D., and Volpe, B., 2006, "Motions or Muscles? Some Behavioral Factors Underlying Robotic Assistance of Motor Recovery," J. Rehabil. Res. Dev., **43**(5), pp. 605–18.

[42] Stienen, A., Hekman, E., van der Helm, F., Prange, G., Jannink, M., Aalsma, A., and van der Kooij, H., 2007, "Dampace: Dynamic Force-Coordination Trainer for the Upper Extremities," *Proceedings of the Tenth ICORR '07*.

[43] Hogan, N., Krebs, H., Charnnarong, J., Srikrishna, P., and Sharon, A., 1992, "MIT-MANUS: A Workstation for Manual Therapy and Training. I," Proceedings of the Second ROMAN '92, pp. 161–165.

[44] Reinkensmeyer, D., Takahashi, C., Timoszyk, W., Reinkensmeyer, A., and Kahn, L., 2001, "Design of Robot Assistance for Arm Movement Therapy Following Stroke," Adv. Rob., **14**(7), pp. 625–637.

[45] Loureiro, R., Amirabdollahian, F., Topping, M., Driessen, B., and Harwin, W., 2003, "Upper Limb Robot Mediated Stroke Therapy—Gentle/s Approach," Auton. Rob., **15**(1), pp. 35–51.

[46] Nakai, A., Ohashi, T., and Hashimoto, H., 1998, "7 DOF Arm Type Haptic Interface for Teleoperation and Virtual Reality Systems," *Proceedings of the IROS '98*, Vol. 2, pp. 1266–1271.

[47] Sanchez, R., Wolbrecht, E., Smith, R., Liu, J., Rao, S., Cramer, S., Rahman, T., Bobrow, J., and Reinkensmeyer, D., 2005, "A Pneumatic Robot for Re-Training Arm Movement After Stroke: Rationale and Mechanical Design," *Proceedings of the Tenth ICORR '05*, pp. 500–504.

[48] Frisoli, A., Rocchi, F., Marcheschi, S., Dettori, A., Salsedo, F., and Bergamasco, M., 2005, "A New Force-Feedback Arm Exoskeleton for Haptic Interaction in Virtual Environments," *Proceedings of the First WHC '05*, pp. 195–201.

[49] Carignan, C., Tang, J., Roderick, S., and Naylor, M., 2007, "A Configuration-Space Approach to Controlling a Rehabilitation Arm Exoskeleton," *Proceedings of the Tenth ICORR '07*.

[50] Perry, J., Rosen, J., and Burns, S., 2007, "Upper-Limb Powered Exoskeleton Design," IEEE/ASME Trans. Mechatron., **12**(4), pp. 408–417.

[51] Mayhew, D., Bachrach, B., Rymer, W., and Beer, R., 2005, "Development of the MACARM—A Novel Cable Robot for Upper Limb Neurorehabilitation," *Proceedings of the Tenth ICORR '05*, pp. 299–302.

[52] Masiero, S., Celia, A., Armani, M., and Rosati, G., 2006, "A Novel Robot Device in Rehabilitation of Post-Stroke Hemiplegic Upper Limbs," Aging Clin. Exp. Res., **18**(6), pp. 531–535.

[53] Stienen, A., Hekman, E., van der Helm, F., Prange, G., Jannink, M., Aalsma, A., and van der Kooij, H., 2007, "Freebal: Dedicated Gravity Compensation for the Upper Extremities," *Proceedings of the Tenth ICORR '07*.

[54] Reinkensmeyer, D., Kahn, L., Averbuch, M., McKenna-Cole, A., Schmit, B., and Rymer, W., 2000, "Understanding and Treating Arm Movement Impairment After Chronic Brain Injury: Progress With the Arm Guide," J. Rehabil. Res. Dev., **37**(6), pp. 653–662.

[55] Colombo, R., Pisano, F., Micera, S., Mazzone, A., Delconte, C., Carrozza, M., Dario, P., and Minuco, G., 2005, "Robotic Techniques for Upper Limb Evaluation and Rehabilitation of Stroke Patients," IEEE Trans. Neural Syst. Rehabil. Eng., **13**(3), pp. 311–324.

[56] Cai, L., Fong, A., Otoshi, C., Liang, Y., Burdick, J., Roy, R., and Edgerton, V., 2006, "Implications of Assist-As-Needed Robotic Step Training After a Complete Spinal Cord Injury on Intrinsic Strategies of Motor Learning," J. Neurosci., **26**(41), pp. 10564–10568.

[57] Kahn, L., Averbuch, M., Rymer, W., and Reinkensmeyer, D., 2001, "Comparison of Robot-Assisted Reaching to Free Reaching in Promoting Recovery From Chronic Stroke," *Proceedings of the Seventh ICORR '01*, pp. 39–44.

[58] Wolbrecht, E., Chan, V., Reinkensmeyer, D., and Bobrow, J., 2008, "Optimizing Compliant, Model-Based Robotic Assistance to Promote Neurorehabilitation," IEEE Trans. Neural Syst. Rehabil. Eng., **16**(3), pp. 286–297.

[59] Bovend'Eerdt, T., Newman, M., Barker, K., Dawes, H., Minelli, C., and Wade,

D., 2008, "The Effects of Stretching in Spasticity: A Systematic Review," Arch. Phys. Med. Rehabil., **89**(7), pp. 1395–1406.

[60] Ellis, M., Sukal, T., and Dewald, J., "Progressive Shoulder Abduction Loading is a Crucial Element of Arm Rehabilitation in Chronic Stroke," Neurorehabil. Neural Repair, in press.

[61] Patton, J., Small, S., and Rymer, W., 2008, "Functional Restoration for the Stroke Survivor: Informing the Efforts of Engineers," Top. Stroke Rehabil., **15**(6), pp. 521–541.

[62] Wu, G., van der Helm, F., Veeger, H., Makhsous, M., van Roy, P., Anglin, C., Nagels, J., Karduna, A., McQuade, K., Wang, X., Werner, F., and Buchholz, B., 2005, "ISB Recommendation on Definitions of Joint Coordinate Systems of Various Joints for the Reporting of Human Joint Motion—Part II: Shoulder, Elbow, Wrist and Hand," J. Biomech., **38**(5), pp. 981–992.

[63] van Ouwerkerk, W., van der Sluijs, J., Nollet, F., Barkhof, F., and Slooff, A., 2000, "Management of Obstetric Brachial Plexus Lesions: State of the Art and Future Developments," Childs Nerv. Syst., **16**(10–11), pp. 638–644.

[64] van Andel, C., Wolterbeek, N., Doorenbosch, C., Veeger, D., and Harlaar, J., 2008, "Complete 3D Kinematics of Upper Extremity Functional Tasks," Gait and Posture, **27**(1), pp. 120–127.

[65] Lenarcic, J., and Stanisic, M., 2003, "A Humanoid Shoulder Complex and the Humeral Pointing Kinematics," IEEE Trans. Rob. Autom., **19**(3), pp. 499–506.

[66] Nef, T., and Riener, R., 2008, "Shoulder Actuation Mechanisms for Arm Rehabilitation Exoskeletons," *Proceedings of the Biorob '08*.

[67] Schiele, A., and van der Helm, F., 2006, "Kinematic Design to Improve Ergonomics in Human Machine Interaction," IEEE Trans. Neural Syst. Rehabil. Eng., **14**(4), pp. 456–469.

[68] Schiele, A., 2008, "An Explicit Model to Predict and Interpret Constraint Force Creation in pHRI With Exoskeletons," *Proceedings of the ICRA '08*, pp. 1324–1330.

[69] Stienen, A., Hekman, E., van der Helm, F., and van der Kooij, H., 2009, "Self-Aligning Exoskeleton Axes Through Decoupling of Joint Rotations and Translations," IEEE Trans. Rob. Autom., **25**(3), pp. 628–633.

[70] Grange, S., Conti, F., Rouiller, P., Helmer, P., and Baur, C., 2001, "The Delta Haptic Device," *Proceedings of the Fifth Mecatronics '01*.

[71] Pratt, G., and Williamson, M., 1995, "Series Elastic Actuators," *Proceedings of the IROS '95*, pp. 399–406.

[72] Robinson, D., 2000, "Design and Analysis of Series Elasticity in Closed-Loop Actuator Force Control," Ph.D. thesis, MIT, Cambridge, MA.

[73] Veneman, J., Ekkelenkamp, R., Kruidhof, R., van der Helm, F., and van der Kooij, H., 2006, "A Series Elastic- and Bowden-Cable-Based Actuation System for Use as Torque Actuator in Exoskeleton-Type Robots," Int. J. Robot. Res., **25**(3), pp. 261–281.

[74] Ekkelenkamp, R., Veltink, P., Stramigioli, S., and van der Kooij, H., 2007, "Evaluation of a Virtual Model Control for the Selective Support of Gait Functions Using an Exoskeleton," *Proceedings of the Tenth ICORR '07*.

[75] Vallery, H., Veneman, J., van Asseldonk, E., Ekkelenkamp, R., Buss, M., and van der Kooij, H., 2008, "Compliant Actuation of Rehabilitation Robots: Benefits and Limitations of Series Elastic Actuators," IEEE Rob. Autom. Mag., **15**(3), pp. 60–69.

[76] Stienen, A., Hekman, E., Schouten, A., van der Helm, F., and van der Kooij, H., "Suitability of Hydraulic Disk Brakes for Passive Actuation of Upper-Extremity Rehabilitation Exoskeletons," Appl. Bionics Biomech., in press.

[77] Jenkins, G., and Watts, D., 1969, *Spectral Analysis and Its Applications*, Holden-Day, San Francisco, CA.

[78] Bendat, J., and Piersol, A., 1986, *Random Data: Analysis and Measurement Procedures*, Wiley, New York.

[79] Simmonds, A., 1991, "Electro-Rheological Valves in a Hydraulic Circuit," IEE Proc.-D: Control Theory Appl., **138**(4), pp. 400–404.

[80] Spencer, B. F., Jr., Dyke, S. J., Sain, M. K., and Carlson, J. D., 1997, "Phenomenological Model for Magnetorheological Dampers," J. Eng. Mech., **123**(3), pp. 230–238.

[81] Sims, N., Holmes, N., and Stanway, R., 2004, "A Unified Modelling and Model Updating Procedure for Electrorheological and Magnetorheological Vibration Dampers," Smart Mater. Struct., **13**(1), pp. 100–121.

[82] Herder, J., 2001, "Energy-Free Systems. Theory, Conception and Design of Statically Balanced Spring Mechanisms," Ph.D. thesis, Delft University of Technology, Delft, The Netherlands.

[83] Barbalace, A., Luchetta, A., Manduchi, G., Moro, M., Soppelsa, A., and Taliercio, C., 2008, "Performance Comparison of VxWorks, Linux, RTAI, and Xenomai in a Hard Real-Time Application," IEEE Trans. Nucl. Sci., **55**(1), pp. 435–439.

[84] Bucher, R., and Balemi, S., 2006, "Rapid Controller Prototyping With MATLAB/ SIMULINK and Linux," Control Eng. Pract., **14**(2), pp. 185–192.

[85] rtai.org

[86] comedi.org

[87] Mitsuhashi, K., Seki, K., Akamatsu, C., and Handa, Y., 2007, "Modulation of Excitability in the Cerebral Cortex Projecting to Upper Extremity Muscles by Rotational Positioning of the Forearm," Tohoku J. Exp. Med., **212**(3), pp. 221–228.

[88] Pratt, J., 1995, "Virtual Model Control of a Biped Walking Robot," Ph.D. thesis, MIT, Cambridge, MA.

[89] Veneman, J., Kruidhof, R., Hekman, E., Ekkelenkamp, R., van Asseldonk, E., and van der Kooij, H., 2007, "Design and Evaluation of the Lopes Exoskeleton Robot for Interactive Gait Rehabilitation," IEEE Trans. Neural Syst. Rehabil. Eng., **15**(3), pp. 379–386.